Neoplasia • Vol. 8, No. 1, January 2006, pp. 31–37 31

www.neoplasia.com

Ad-IRF-1 Induces Apoptosis in Esophageal Adenocarcinoma

Gregory A. Watson[*,1], Pierre E. Queiroz de Oliveira*[*,1], Michael T. Stang*, Michaele J. Armstrong*, William E. Gooding*[†], Shih-Fan Kuan*[‡], John H. Yim* and Steven J. Hughes**

Departments of *Surgery, [†]Biostatistics, and [‡]Pathology, University of Pittsburgh, Pittsburgh, PA, USA

Abstract

The nuclear transcription factor interferon regulatory factor-1 (IRF-1) is a putative tumor suppressor, but the expression and function of IRF-1 in esophageal adenocarcinoma (EA) remain unknown. We hypothesized that IRF-1 expression was reduced or lost in EA and that restoration of IRF-1 would result in the apoptosis of EA cells *in vitro* and the inhibition of tumor growth *in vivo*. Three EA cell lines were used to examine IRF-1 expression, IFN-γ responsiveness, and the effects of IRF-1 overexpression using a recombinant adenoviral vector (Ad-IRF-1). All three EA cell lines produced IRF-1 protein following IFN-γ stimulation, although IFN-γ did not induce cell death. In contrast, Ad-IRF-1 infection resulted in high levels of IRF-1 protein and triggered apoptosis in all three EA cell lines. Potential mechanisms for the differential response to IFN-γ *versus* Ad-IRF-1—such as modulation of c-Met or extracellular regulated kinase signaling, or altered expression of IRF-2, Fas, or survivin—were investigated, but none of these mechanisms can account for this observation. *In vivo* administration of IRF-1 in a murine model of EA modestly inhibited tumor growth, but did not lead to tumor regression. Strategies aimed at increasing or restoring IRF-1 expression may have therapeutic benefits in EA.

Neoplasia (2006) **8,** 31–37

Keywords: Interferon regulatory factor-1 (IRF-1), interferon gamma (IFN-γ), Fas, c-Met, hepatocyte growth factor.

Introduction

The nuclear transcription factor interferon regulatory factor-1 (IRF-1) has been implicated as a potential tumor suppressor [1–5]. IRF-1 is primarily induced by interferon gamma (IFN-γ), but is also induced by IFN-α, IFN-β, tumor necrosis factor-α, retinoic acid, interleukin (IL) 1, and IL-6 [1,2,6–8]. IFN-γ leads to the activation of Janus kinase-1 (Jak-1) and Jak-2, resulting in the phosphorylation and dimerization of signal transducer and activator of transcription-1 (STAT-1). STAT-1 homodimers then translocate to the nucleus and bind to promoter IFN-γ activation site elements to initiate or suppress the transcription of IFN-γ–regulated genes such as *IRF-1* [9]. IRF-1 subsequently binds to specific DNA sequences in several promoters (IFN-stimulated response element) to initiate the transcription of genes involved in mediating the antiviral, immunomodulatory, antiproliferative, and apoptotic effects of IFN-γ signaling [2,10,11].

There have been few studies demonstrating the role of IRF-1 in the pathology and treatment of gastrointestinal malignancies [5,12], and there have been no studies examining IRF-1 in esophageal adenocarcinoma (EA). The incidence of EA is rising more rapidly than any other tumor; currently, EA represents the most common histologic type of esophageal cancer in the United States [13–15]. Despite advances in diagnosis and treatment, overall 5-year survival remains approximately 14% [16]. Given its potential tumor-suppressor capabilities, we evaluated IRF-1 expression and IFN-γ responsiveness in three EA cell lines and examined the effects of IRF-1 overexpression on EA cell viability and tumor growth rates. Our findings demonstrate that Ad-IRF-1 infection of EA cells induces apoptosis *in vitro* and modestly inhibits tumor growth rates *in vivo*.

Materials and Methods

Cell Lines

Three human EA-derived cell lines (Seg-1, Bic-1, and Flo-1) have been previously described [17]. Seg-1 was maintained in RPMI 1640, and Bic-1 and Flo-1 were maintained in DMEM (BioWhittaker, Walkersville, MD). Media were supplemented with 10% fetal bovine serum (Atlanta Biologicals, Norcross, GA), 1% penicillin/streptomycin, and 1% L-glutamine (Invitrogen, Carlsbad, CA), and cells were propagated in a humidified environment at 37°C with 5% CO_2.

Antibodies and Reagents

For immunoblotting, anti-human IRF-1, anti-murine IRF-1, anti-Fas (C-20), anti–phospho extracellular regulated kinase (ERK), anti-ERK, and anti–IRF-2 antibodies were purchased from Santa Cruz Biotechnology, Inc. (Santa Cruz, CA). Anti-survivin antibody and human IFN-γ were purchased from R&D Systems (Minneapolis, MN). Anti-Fas antibody Apo 1-1 was purchased from Kamiya Biomedical Co. (Seattle, WA). Secondary antibodies were purchased from Jackson Immunoresearch, Inc. (West Grove, PA). zVad was purchased from Promega

Address all correspondence to: Steven J. Hughes, 497 Scaife Hall, 3550 Terrace Street, Pittsburgh, PA 15261. E-mail: hughess2@upmc.edu

[1]Gregory A. Watson and Pierre E. Queiroz de Oliveira contributed equally to this work.

Received 25 August 2005; Revised 31 October 2005; Accepted 31 October 2005.

DOI 10.1593/neo.05559

(Madison, WI). The ERK inhibitor PD98059 (50 μM) was purchased from Calbiochem (La Jolla, CA). The c-Met–specific inhibitor PHA665752 (200 nM) [18] was provided by James Christensen (Pfizer, San Francisco, CA).

Ad-IRF-1 Construction and Infection

The Ad-IRF-1 construct has previously been described [19]. Cells were infected for 4 hours at 37°C in 5% CO_2 with either empty adenovirus (Ad-Ψ5) or murine IRF-1 construct (Ad-IRF-1). Optimal multiplicity of infection (MOI) was determined by using Ad-eGFP and by measuring the percentage of fluorescent cells 24 and 48 hours later. Approximately 90% transduction was achieved with MOI = 100 in Seg-1 and Flo-1 and with MOI = 500 in Bic-1.

Immunoblotting

Cellular protein was extracted using lysis buffer (Cell Signaling Technology, Beverly, MA) containing 1 mM phenylmethlsulfonylfluoride (Sigma-Aldrich Corp., Atlanta, GA) and quantified using BCA protein assay kit (Pierce, Rockford, IL). Proteins were resolved using sodium dodecyl sulfate (SDS) polyacrylamide gels and subsequently transferred to nitrocellulose membranes (Bio-Rad, Hercules, CA). Membranes were blocked in 5% milk solution, incubated with primary antibody, washed, and incubated with HRP-conjugated secondary antibody. Immunoreactivity was detected using Supersignal West Pico Chemiluminescent Substrate (Pierce) and X-ray film (Eastman Kodak, Rochester, NY). Blots were stripped with 2% SDS, 100 mM β-mercaptoethanol, and 62.5 mM Tris (pH 6.8) for 20 minutes at 60°C and reprobed with anti–β-actin (Sigma-Aldrich Corp.).

FACScan Analysis of Apoptosis and Fas Expression

Cells were treated with a supraphysiologic dose of human IFN-γ (1,000 U/ml) or infected with Ad-Ψ5 or Ad-IRF-1, as above. For apoptosis studies, the pan-caspase inhibitor zVad (50 μM) was added to the cultures following a 4-hour infection period, and the cells were propagated for 36 hours, harvested, and stained using Annexin V (AV)-fluorescein isothiocyanate (FITC) apoptosis detection kit (BD Biosciences, San Diego, CA). For Fas cell surface expression, cells were collected and rinsed at various time points (0.5–36 hours), as above. Cells were labeled with Apo 1-1 anti-Fas antibody and FITC-conjugated secondary antibody. Apoptosis and Fas expressions were assessed by flow cytometry using a Becton Dickinson FACSort (San Jose, CA).

In Vivo *Treatment of Tumor-Bearing Mice*

All animal studies were conducted in accordance with the Council on Animal Care at the University of Pittsburgh (Pittsburgh, PA). Seg-1 cells growing in log phase were resuspended in Hanks balanced salt solution, and 2.5×10^6 cells were inoculated subcutaneously in the right flank of 4- to 6-week-old male nude nu/nu-nubr mice (Charles River Laboratories, Wilmington, MA). When tumors reached 30 to 35 mm^3 by perpendicular measurements, mice were randomized ($n = 5$ mice per group) and received intratumoral injection of 6×10^8 plaque-forming units of Ad-IRF-1, Ad-Ψ5, or PBS (in a total volume of 30 μl) every 4 days for a total of three treatments. Tumor growth was followed by serial measurements of perpendicular diameters using digital calipers. Tumor volumes were calculated according to the formula: $0.52 \times (\text{width})^2 \times \text{length}$ [20]. Animals that were moribund or had tumors greater than approximately 4189 mm^3 were sacrificed.

Statistical Analysis

In vivo tumor growth rates for each treatment group were compared by estimating tumor growth curves (after regressing log-transformed tumor volumes on each day's tumor volume measurement) and by testing differences in regression coefficients. A mixed-model approach [21], which represents individual mice as random effects and accounts for between- and within-mouse variations, was used. A likelihood ratio test was constructed to determine the appropriate choice for model parameters. In addition to model-based results, differences in means on day 10 (as a check for adequacy of randomization) and day 26 (final day of tumor measurements) were tested with Kruskal-Wallis test [22].

Results

IFN-γ Signaling Pathway Is Intact in EA Cells

We began our study by characterizing IRF-1 expression and the IFN-γ signaling pathway in three EA cell lines. By immunoblot analysis, Bic-1, Seg-1, and Flo-1 cells lack detectable IRF-1 protein in the absence of IFN-γ stimulation (Figure 1*A*). All three EA cell lines express IRF-1 protein following IFN-γ stimulation, with peak levels observed at 24 hours in the Seg-1 and Flo-1 cell lines and at 48 hours in the Bic-1 cell line. IRF-1 protein expression persists for 72 hours following IFN-γ stimulation in all of the EA cell lines, except for Seg-1, where IRF-1 protein is undetectable at 48 hours. Obvious morphologic changes or signs of cell death were not seen, even after 72 hours of stimulation with IFN-γ (data not shown). We concluded that IRF-1 protein is expressed in all three EA cell lines following IFN-γ stimulation, suggesting that *IRF-1* is not lost and that the IFN-γ signaling pathway is intact.

Next, we overexpressed IRF-1 in the EA cell lines using an adenoviral IRF-1 vector, which was previously shown to result in the production of murine IRF-1 that is functional in human cells [19]. Figure 1*B* demonstrates that IRF-1 protein was expressed in all three EA cell lines 24 hours following infection with Ad-IRF-1. Infection with an empty adenovirus (Ad-Ψ5) did not induce IRF-1 expression. Near-complete loss of cultures was observed following Ad-IRF-1 infection, suggesting treatment-induced cell death (data not shown). These results demonstrate that Ad-IRF-1 infection results in abundant IRF-1 protein expression. In contrast to IFN-γ treatment, Ad-IRF-1 infection appears to induce extensive cell death in these EA cell lines.

Ad-IRF-1 Infection Induces Apoptosis in EA Cells

IRF-1 has previously been shown to induce apoptosis in other cell types [4,19,23,24]. Because Ad-IRF-1 infection

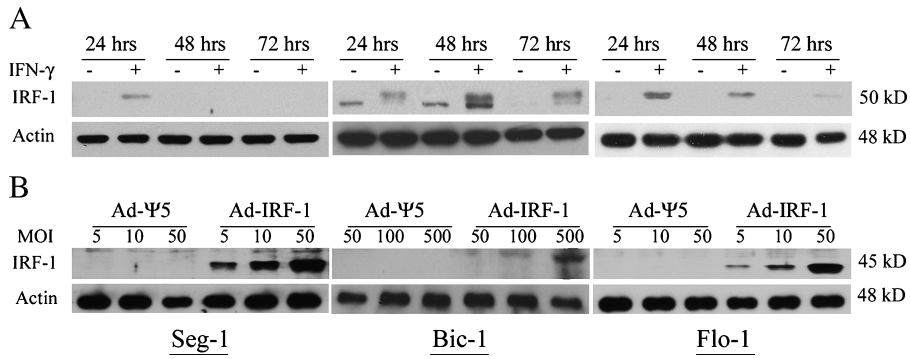

Figure 1. *The IFN-γ signaling pathway is intact in EA cells. (A) Three EA cell lines (Seg-1, Bic-1, and Flo-1) were cultured for 24 to 72 hours in the presence or absence of human IFN-γ (1,000 U/ml). IFN-γ induced human IRF-1 (50 kDa) expression in all three EA cell lines. The smaller band seen in the untreated Bic-1 cell line is inconsistently observed in all three EA cell lines regardless of treatment and is suspected to represent nonspecific immunoreactivity. (B) Seg-1, Bic-1, and Flo-1 EA cell lines were infected at a range of MOI with either an empty adenoviral vector (Ad-Ψ5) or Ad-IRF-1. Ad-IRF-1 (but not Ad-Ψ5) resulted in an MOI-dependent increase in murine IRF-1 (45 kDa) expression.*

caused near-complete loss of cultures, we hypothesized that Ad-IRF-1 infection induced apoptosis. Thirty-six hours following infection with either Ad-Ψ5 or Ad-IRF-1, cell viability was analyzed using flow cytometry. We observed a substantial increase in positively stained cell populations following Ad-IRF-1 infection, but not following IFN-γ treatment (Figure 2*A*). This effect was not observed in the cultures treated with equivalent MOI of Ad-Ψ5, suggesting that it is due to IRF-1 expression and not nonspecific viral-induced necrosis. This effect was seen within 24 hours of infection, and the maximum percentage of nonviable cells was observed at 48 hours in all three EA cell lines. Pretreatment with the pan-caspase inhibitor zVad rescued a variable percentage of the cells from Ad-IRF-1–induced cell death (Figure 2, *A* and *B*), suggesting that Ad-IRF-1–induced cell death is, in large part, due to apoptosis. This was further supported by demonstrations of PARP cleavage and induced caspase-3 activity (data not shown). Taken together, these findings show that Ad-IRF-1 infection (but not IFN-γ treatment) induces significant apoptosis in EA cells.

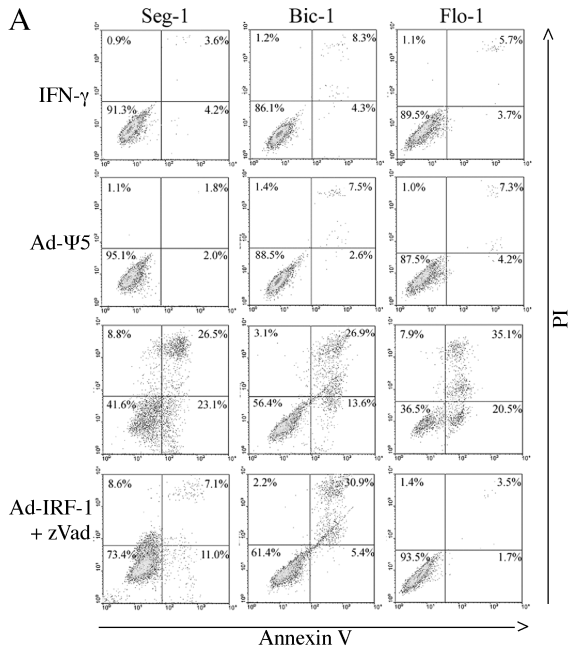

B

% VIABLE CELLS			
	Seg-1	*Bic-1*	*Flo-1*
IFN-gamma	91.3%	86.1%	89.5%
AD-psi5	95.1%	88.5%	87.5%
AD-IRF-1	41.6%	56.4%	36.5%
Ad-IRF-1 + zVad	73.4%	61.4%	93.5%
% zVad Rescue	31.8%	5.0%	57.0%

Figure 2. *Ad-IRF-1 infection induces apoptosis in EA cells. (A) FACScan analysis of AV- and propidium iodide (PI)–stained cells 36 hours following treatment with a supraphysiologic dose (1,000 U/ml) of IFN-γ or infection with either empty adenovirus (Ad-Ψ5) or Ad-IRF-1. Positive staining for AV suggests apoptosis (right lower quadrant). Positive staining for PI suggests loss of membrane integrity late in apoptosis (right upper quadrant) or necrosis (left upper quadrant). Neither treatment with IFN-γ nor infection with Ad-Ψ5 resulted in significant apoptosis. Ad-IRF-1 infection caused cell death in all three EA cell lines, which was largely prevented by pretreatment with the pan-caspase inhibitor zVad, suggesting that Ad-IRF-1 induces apoptosis. (B) Percentage of viable cells corresponds to the negatively stained population (left lower quadrant). Percent zVad rescue represents the difference between the viable populations following infection with Ad-IRF-1 in the presence or absence of zVad.*

EA Cells Produce Functional IRF-1 Following IFN-γ Stimulation

Several key mediators of apoptosis, including the death receptor Fas, the IRF-1 antagonist IRF-2, and the inhibitor-of-apoptosis protein survivin, are known targets of IFN-γ signaling [4,25–27]. Because Ad-IRF-1 infection (but not IFN-γ treatment) induced apoptosis, we hypothesized that modulation of these mediators by Ad-IRF-1 and IFN-γ differed. Cell surface Fas expression increased to a similar degree following treatment with both IFN-γ and Ad-IRF-1 (Figure 3*A*). This effect was evident by 12 hours and persisted for 36 hours in IFN-γ–treated (but not Ad-IRF-1–infected)

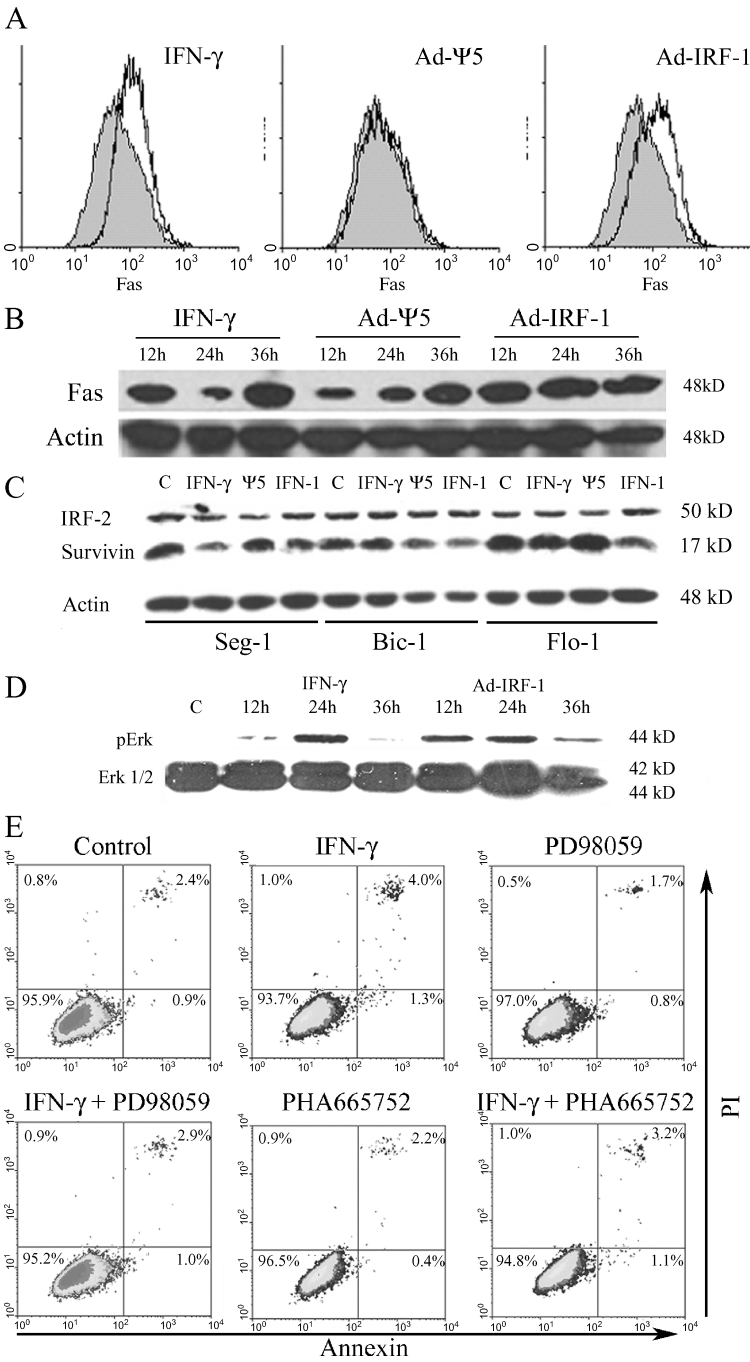

Figure 3. *Effects of IFN-γ stimulation compared to Ad-IRF-1 infection. (A) FACScan and (B) immunoblotting of Fas expression in Seg-1 cells following treatment with either IFN-γ (1,000 U/ml), Ad-Ψ5, or Ad-IRF-1. Although Fas protein increased following all three treatments, only IFN-γ and Ad-IRF-1 resulted in increased cell surface expression of Fas (shaded histograms represent controls; 24-hour time point shown). (C) Immunoblot for IRF-2 and survivin 36 hours following treatment with IFN-γ, Ad-Ψ5, or Ad-IRF-1. Neither treatment altered IRF-2 levels. Survivin levels decreased modestly following Ad-IRF-1 infection (but not IFN-γ treatment) in Bic-1 and Flo-1 cells, whereas survivin decreased following IFN-γ treatment (but not Ad-IRF-1 infection) in Seg-1 cells. (D) ERK2 is phosphorylated (pErk) in Seg-1 cells following treatment with both IFN-γ and Ad-IRF-1. Total ERK levels were unchanged. (E) FACScan analysis of AV- and PI-labeled Seg-1 cells treated with IFN-γ for 72 hours in the presence or absence of the ERK inhibitor PD98059 (50 μM) or the c-Met inhibitor PHA665752 (200 nM). Neither ERK inhibition nor c-Met inhibition sensitized the cells to IFN-γ.*

cells. Fas protein increased following all treatments, including Ad-Ψ5 (Figure 3*B*), suggesting that increased Fas cell surface expression is not due to increased protein synthesis alone. Neither IFN-γ treatment nor Ad-IRF-1 infection altered IRF-2 expression (Figure 3*C*). Survivin levels consistently decreased following IFN-γ treatment, but not following Ad-IRF-1 infection in Seg-1 cells, whereas the converse was true in Bic-1 and Flo-1 cells (Figure 3*C*), suggesting that modulation of survivin is cell line–specific and that decreased survivin levels alone are not sufficient to induce apoptosis in Seg-1 cells. We concluded that the discrepancy between the ability of IFN-γ and Ad-IRF-1 to induce apoptosis in these EA cells is not solely related to differential modulation of these apoptotic mediators.

IFN-γ stimulation also activates pathways that antagonize apoptosis, including ERK2 [28] and c-Met [29,30], and we have previously shown universal overexpression of the hepatocyte growth factor receptor c-Met in EA [31]. We hypothesized that IFN-γ treatment (but not Ad-IRF-1 infection) would activate ERK2 and c-Met signaling. Interestingly, both IFN-γ and Ad-IRF-1 resulted in varying degrees of ERK2 phosphorylation (Figure 3*D*), but inhibition of ERK2 combined with IFN-γ treatment did not induce apoptosis (Figure 3*E*). Likewise, inhibition of c-Met with PHA665752 did not sensitize these EA cells to IFN-γ (Figure 3*E*). We concluded that IRF-1 at least partially modulates IFN-γ–induced activation of ERK2, but that neither ERK2 nor c-Met signaling regulates IFN-γ sensitivity in these EA cells. Taken together, these findings suggest that IRF-1 produced following IFN-γ stimulation is functional and that activation of an undefined pathway may mediate IFN-γ responsiveness in these EA cells.

In Vivo *Administration of Ad-IRF-1 Decreases Tumor Growth Rates*

Given our *in vitro* findings demonstrating that IRF-1 induces apoptosis in EA cells, we hypothesized that Ad-IRF-1 injection into established flank tumors in nude mice would result in tumor regression. Figure 4 demonstrates observed (dotted) and predicted (solid) growth rates of tumors measured every 3 to 4 days following treatment. There were no differences in mean tumor volumes on the first day of tumor measurements (day 10; $P = .763$) or on the final day of measurement (day 26; $P = .618$). A mixed quadratic model was fitted to log-transformed tumor volumes. A test for equality of slopes revealed modest evidence of interaction between treatment groups (PBS, Ad-Ψ5, and Ad-IRF-1) and day of measurement ($P = .062$), suggesting unequal regression coefficients and differential tumor growth rates. The apparent difference in growth rate may be attributed to a decrease in growth rate for Ad-IRF-1–treated mice. No negative effects of the treatment, such as local skin ulcers, reduction in activity, or decreased enteral intake, were observed in any of the mice. Tumors were resected at the conclusion of the experiment and analyzed for IRF-1 expression by immunostaining. IRF-1 immunoreactivity was not observed in either treatment group (data not shown). This was expected given the known rapid clearance of IRF-1–transduced cells *in vivo* [27]. These results demonstrate that intratumoral delivery of Ad-IRF-1 modestly inhibits tumor growth rates in an *in vivo* model of EA, but does not lead to tumor regression.

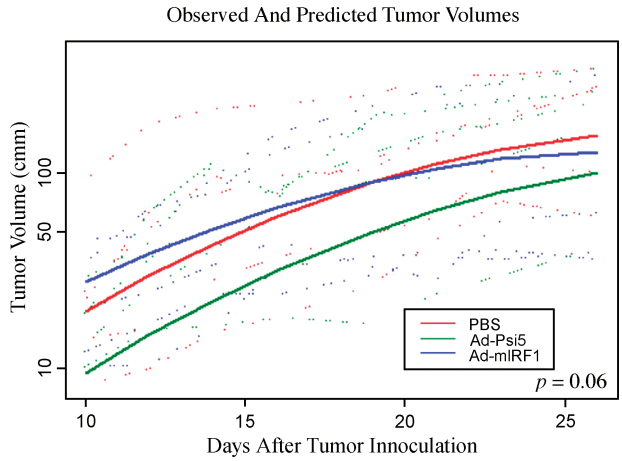

Figure 4. *Differential growth rate of tumors* in vivo *derived from Seg-1 cells following intratumoral injection with PBS, Ad-Ψ5, or Ad-IRF-1. The graph shows observed and predicted tumor volumes of five mice randomly assigned to treatment with PBS, control vector (Ad-Ψ5), or Ad-IRF-1. The dotted lines are the observed tumor volumes; the solid lines are the predicted tumor volumes based on the fitted model. Ad-IRF-1 treatment modestly inhibited tumor growth rates (P = 0.06) but did not result in regression.*

Discussion

Our study is one of the few to investigate the role of IRF-1 in the pathophysiology and treatment of gastrointestinal malignancies and is the first to examine its role in EA. We have shown that IRF-1 overexpression induces apoptosis in EA cells *in vitro* and inhibits EA tumor growth rates *in vivo*. Little, if any, basal IRF-1 protein was detected in these EA cells, but all three cell lines expressed IRF-1 following IFN-γ stimulation, suggesting that *IRF-1* is not lost and that the IFN-γ signaling pathway is functional. A supraphysiologic dose of IFN-γ did not induce cell death, yet Ad-IRF-1 infection induced extensive apoptosis in all three cell lines. Additionally, *in vivo* administration of Ad-IRF-1 in a murine model of EA resulted in decreased rates of tumor growth relative to controls. Taken together, these findings support the use of strategies to augment IRF-1 expression as a therapeutic option for EA.

Studies in breast cancer have shown that IRF-1 expression is reduced or lost both *in vitro* and *in vivo* [32]. Similarly, we observed little, if any, IRF-1 expression in unstimulated EA cells. Ad-IRF-1 infection generates high levels of functional IRF-1 protein and induces apoptosis in breast cancer [19,27] and other neoplasms [2]. Indeed, Ad-IRF-1 infection induced substantial apoptosis *in vitro* in two of the EA cell lines (Seg-1 and Flo-1), with lesser effects seen in Bic-1 cells. This finding may be attributable to reduced postinfection IRF-1 production in Bic-1 cells relative to Seg-1 and Flo-1 cells (Figure 1*B*). The possibility that Bic-1 cells are less sensitive to the effects of Ad-IRF-1, however, must be considered. Importantly, this Ad-IRF-1 induction of apoptosis is in contrast to our previous experience with other virally introduced proteins such as Ad-p53 that have not resulted in the induction of apoptosis [33].

Although IFN-γ treatment alone induces apoptosis in some carcinoma models [12,34], resistance to IFN-γ is common. Levels of IRF-1 may determine whether IFN-γ induces apoptosis, and the amount of IRF-1 produced following IFN-γ treatment may be regulated by the amount of IFN-γ receptor (IFNGR) present [35,36] or the rapid downregulation of IFNGR. Lack of IRF-1 expression in Seg-1 cells 48 hours following IFN-γ stimulation (Figure 1*A*) suggests that rapid downregulation of the IFNGR may occur in this cell line. Although it remains possible that Ad-IRF-1 infection generates more IRF-1 than IFN-γ treatment, we did not observe a significant difference in the transduction of known targets of IRF-1 (i.e., Fas) between the two treatments.

IFN-γ stimulation is also known to generate antagonistic effects simultaneous to those of IRF-1 (i.e., IRF-2), or to activate pathways that oppose IRF-1 function (i.e., c-Met and ERK2). IRF-2 is a putative oncogene and antagonizes IRF-1 by competing for the same DNA-binding sites [37]. All three of our EA cell lines abundantly express IRF-2 (Figure 3*C*); although IRF-2 levels were not altered by IFN-γ or Ad-IRF-1, overexpression of IRF-2 may inhibit responsiveness to IFN-γ in these cell lines. c-Met and ERK activation typically results in cell proliferation and resistance to apoptosis [38,39], although our observations fail to support a significant role for c-Met or ERK in the regulation of IFN-γ sensitivity. Collectively, our data suggest that other signaling events downstream of the IFNGR may counter IFN-γ signaling through STAT-1.

Although inhibition of tumor growth rates following Ad-IRF-1 treatment *in vivo* did not reach statistical significance, a trend was apparent. Although repetition of *in vivo* experiments with more animals, larger doses of Ad-IRF-1, or smaller tumor burdens at the onset may have produced statistically significant results, we have not pursued this, as our current data suggest that replication-deficient adenoviral delivery through direct tumor injection will not produce an adequate clinical response to an established tumor [40]. Rather, we conclude that alternative viral delivery strategies need to be considered (i.e. retrovirus).

In summary, our study is the first to investigate the role of IRF-1 in the pathophysiology and treatment of EA. We have shown that IRF-1 overexpression induces the apoptosis of EA cells *in vitro* and modestly inhibits tumor growth rates *in vivo*. Taken together, our findings suggest that strategies designed to augment IRF-1 expression may be useful in the management of EA.

References

[1] Yim JH, Wu SJ, Casey MJ, Norton JA, and Doherty GM (1997). IFN regulatory factor-1 gene transfer into an aggressive, nonimmunogenic sarcoma suppresses the malignant phenotype and enhances immunogenicity in syngeneic mice. *J Immunol* **158,** 1284–1292.

[2] Kroger A, Koster M, Schroeder K, Hauser H, and Mueller PP (2002). Activities of IRF-1. *J Interferon Cytokine Res* **22,** 5–14.

[3] Kroger A, Dallugge A, Kirchhoff S, and Hauser H (2003). IRF-1 reverts the transformed phenotype of oncogenically transformed cells *in vitro* and *in vivo*. *Oncogene* **22,** 1045–1056.

[4] Tomita Y, Bilim V, Hara N, Kasahara T, and Takahashi K (2003). Role of IRF-1 and caspase-7 in IFN-gamma enhancement of Fas-mediated apoptosis in ACHN renal cell carcinoma cells. *Int J Cancer* **104,** 400–408.

[5] Beppu K, Morisaki T, Matsunaga H, Uchiyama A, Ihara E, Hirano K, Kanaide H, Tanaka M, and Katano M (2003). Inhibition of interferon-gamma–activated nuclear factor-kappa B by cyclosporin A: a possible mechanism for synergistic induction of apoptosis by interferon-gamma and cyclosporin A in gastric carcinoma cells. *Biochem Biophys Res Commun* **305,** 797–805.

[6] Fujita T, Kimura Y, Miyamoto M, Barsoumian EL, and Taniguchi T (1989). Induction of endogenous IFN-alpha and IFN-beta genes by a regulatory transcription factor, IRF-1. *Nature* **337,** 270–272.

[7] Geller DA, Nguyen D, Shapiro RA, Nussler A, Di Silvio M, Freeswick P, Wang SC, Tweardy DJ, Simmons RL, and Billiar TR (1993). Cytokine induction of interferon regulatory factor-1 in hepatocytes. *Surgery* **114,** 235–242.

[8] Harroch S, Revel M, and Chebath J (1994). Induction by interleukin-6 of interferon regulatory factor 1 (*IRF-1*) gene expression through the palindromic interferon response element pIRE and cell type–dependent control of IRF-1 binding to DNA. *EMBO J* **13,** 1942–1949.

[9] Schroder K, Hertzog PJ, Ravasi T, and Hume DA (2004). Interferon-gamma: an overview of signals, mechanisms and functions. *J Leukoc Biol* **75,** 163–189.

[10] Ossina NK, Cannas A, Powers VC, Fitzpatrick PA, Knight JD, Gilbert JR, Shekhtman EM, Tomei LD, Umansky SR, and Kiefer MC (1997). Interferon-gamma modulates a p53-independent apoptotic pathway and apoptosis-related gene expression. *J Biol Chem* **272,** 16351–16357.

[11] Tamura T, Ueda S, Yoshida M, Matsuzaki M, Mohri H, and Okubo T (1996). Interferon-gamma induces ice gene expression and enhances cellular susceptibility to apoptosis in the U937 leukemia cell line. *Biochem Biophys Res Commun* **229,** 21–26.

[12] Detjen KM, Farwig K, Welzel M, Wiedenmann B, and Rosewicz S (2001). Interferon gamma inhibits growth of human pancreatic carcinoma cells *via* caspase-1 dependent induction of apoptosis. *Gut* **49,** 251–262.

[13] Devesa SS, Blot WJ, Fraumeni JF Jr (1998). Changing patterns in the incidence of esophageal and gastric carcinoma in the United States. *Cancer* **83,** 2049–2053.

[14] Blot WJ, Devesa SS, Kneller RW, Fraumeni JF Jr (1991). Rising incidence of adenocarcinoma of the esophagus and gastric cardia. *JAMA* **265,** 1287–1289.

[15] Blot WJ and McLaughlin JK (1999). The changing epidemiology of esophageal cancer. *Semin Oncol* **26,** 2–8.

[16] Greenlee RT, Hill-Harmon MB, Murray T, and Thun M (2001). Cancer statistics, 2001 (vol 51, p 15, 2001). *Ca Cancer J Clin* **51,** 373.

[17] Hughes SJ, Nambu Y, Soldes OS, Hamstra D, Rehemtulla A, Iannettoni MD, Orringer MB, and Beer DG (1997). Fas/APO-1 (CD95) is not translocated to the cell membrane in esophageal adenocarcinoma. *Cancer Res* **57,** 5571–5578.

[18] Christensen JG, Burrows J, and Salgia R (2005). c-Met as a target for human cancer and characterization of inhibitors for therapeutic intervention. *Cancer Lett* **225,** 1–26.

[19] Kim PK, Armstrong M, Liu Y, Yan P, Bucher B, Zuckerbraun BS, Gambotto A, Billiar TR, and Yim JH (2004). IRF-1 expression induces apoptosis and inhibits tumor growth in mouse mammary cancer cells *in vitro* and *in vivo*. *Oncogene* **23,** 1125–1135.

[20] Tomayko MM and Reynolds CP (1989). Determination of subcutaneous tumor size in athymic (nude) mice. *Cancer Chemother Pharmacol* **24,** 148–154.

[21] Zeger SL and Diggle PJ (1994). Semiparametric models for longitudinal data with application to CD4 cell numbers in HIV seroconverters. *Biometrics* **50,** 689–699.

[22] Hollander M and Wolfe DA (1999). Nonparametric Statistical Methods, 2nd ed John Wiley and Sons, New York.

[23] Kim EJ, Lee JM, Namkoong SE, Um SJ, and Park JS (2002). Interferon regulatory factor-1 mediates interferon-gamma–induced apoptosis in ovarian carcinoma cells. *J Cell Biochem* **85,** 369–380.

[24] Kano A, Haruyama T, Akaike T, and Watanabe Y (1999). IRF-1 is an essential mediator in IFN-gamma–induced cell cycle arrest and apoptosis of primary cultured hepatocytes. *Biochem Biophys Res Commun* **257,** 672–677.

[25] Inaba H, Glibetic M, Buck S, Ravindranath Y, and Kaplan J (2004). Interferon-gamma sensitizes osteosarcoma cells to Fas-induced apoptosis by up-regulating Fas receptors and caspase-8. *Pediatr Blood Cancer* **43,** 729–736.

[26] Yim JH, Ro SH, Lowney JK, Wu SJ, Connett J, and Doherty GM (2003). The role of interferon regulatory factor-1 and interferon regulatory factor-2 in IFN-gamma growth inhibition of human breast carcinoma cell lines. *J Interferon Cytokine Res* **23,** 501–511.

[27] Pizzoferrato E, Liu Y, Gambotto A, Armstrong MJ, Stang MT, Gooding WE, Alber SM, Shand SH, Watkins SC, Storkus WJ, et al. (2004).

Ectopic expression of interferon regulatory factor-1 promotes human breast cancer cell death and results in reduced expression of survivin. *Cancer Res* **64,** 8381–8388.

[28] David M, Petricoin E III, Benjamin C, Pine R, Weber MJ, and Larner AC (1995). Requirement for MAP kinase (ERK2) activity in interferon alpha- and interferon beta–stimulated gene expression through STAT proteins. *Science* **269,** 1721–1723.

[29] Gohda E, Takebe T, Sotani T, Nakamura S, Minowada J, and Yamamoto I (1998). Induction of hepatocyte growth factor/scatter factor by interferon-gamma in human leukemia cells. *J Cell Physiol* **174,** 107–114.

[30] Takami Y, Yamamoto I, Tsubouchi H, and Gohda E (2005). Modulation of hepatocyte growth factor induction in human skin fibroblasts by retinoic acid. *Biochim Biophys Acta* **1743,** 49–56.

[31] Herrera LJ, El Hefnawy T, Queiroz de Oliveira PE, Raja S, Finkelstein S, Gooding W, Luketich JD, Godfrey TE, and Hughes SJ (2005). The HGF receptor c-Met is overexpressed in esophageal adenocarcinoma. *Neoplasia* **7,** 75–84.

[32] Doherty GM, Boucher L, Sorenson K, and Lowney J (2001). Interferon regulatory factor expression in human breast cancer. *Ann Surg* **233,** 623–629.

[33] Mahidhara RS, Queiroz de Oliveira PE, Kohout J, Beer DG, Lin J, Watkins SC, Robbins PD, and Hughes SJ (2005). Altered trafficking of Fas and subsequent resistance to Fas-mediated apoptosis occurs by a wild-type p53 independent mechanism in esophageal adenocarcinoma. *J Surg Res* **123,** 302–311.

[34] Detjen KM, Kehrberger JP, Drost A, Rabien A, Welzel M, Wiedenmann B, and Rosewicz S (2002). Interferon-gamma inhibits growth of human neuroendocrine carcinoma cells *via* induction of apoptosis. *Int J Oncol* **21,** 1133–1140.

[35] Bernabei P, Allione A, Rigamonti L, Bosticardo M, Losana G, Borghi I, Forni G, and Novelli F (2001). Regulation of interferon-gamma receptor (INF-gammaR) chains: a peculiar way to rule the life and death of human lymphocytes. *Eur Cytokine Netw* **12,** 6–14.

[36] Burke F, Smith PD, Crompton MR, Upton C, and Balkwill FR (1999). Cytotoxic response of ovarian cancer cell lines to IFN-gamma is associated with sustained induction of IRF-1 and p21 mRNA. *Br J Cancer* **80,** 1236–1244.

[37] Yim JH, Wu SJ, Lowney JK, Vander Velde TL, and Doherty GM (1999). Enhancing *in vivo* tumorigenicity of B16 melanoma by overexpressing interferon regulatory factor-2: resistance to endogenous IFN-gamma. *J Interferon Cytokine Res* **19,** 723–729.

[38] Gao CF and Vande Woude GF (2005). HGF/SF-Met signaling in tumor progression. *Cell Res* **15,** 49–51.

[39] Lewis TS, Shapiro PS, and Ahn NG (1998). Signal transduction through MAP kinase cascades. *Adv Cancer Res* **74,** 49–139.

[40] Rochlitz CF (2001). Gene therapy of cancer. *Swiss Med Wkly* **131,** 4–9.